AIAA'89

AIAA 89-1049
Noise Reduction of a Composite Cylinder Subjected to Random Acoustic Excitation

F. Grosveld and T. Beyer
NASA-Langley
Hampton, VA

AIAA 12th Aeroacoustics Conference

April 10–12, 1989 / San Antonio, TX

For permission to copy or republish, contact the American Institute of Aeronautics and Astronautics
370 L'Enfant Promenade, S.W., Washington, D.C. 20024

NOISE REDUCTION OF A COMPOSITE CYLINDER SUBJECTED TO RANDOM ACOUSTIC EXCITATION

Ferdinand W. Grosveld*
Planning Research Corporation
Hampton, Virginia 23666

Abstract

Interior and exterior noise measurements have been performed on a stiffened, composite, floor-equipped cylinder. Noise reduction has been obtained for the case of random acoustic excitation in a diffuse field. The frequency range of interest was 100 Hz - 800 Hz one-third octave bands. Measurements were conducted on the cylinder with and without an interior trim installed. The interior trim consisted of a thin layer of lead sandwiched between two 0.25 inch thick layers of foam. The trim was installed on the ring stiffeners inside the cylinder leaving a 2 inch airgap. The measured data were compared with noise reduction predictions from the Propeller Aircraft Interior Noise (PAIN) program and from a Statistical Energy Analysis (SEA). Structural modal parameters were not predicted well by the PAIN program for the given input parameters. This resulted in incorrect noise reduction predictions for the lower one-third octave bands where the power flow into the interior of the cylinder was predicted on a mode-per-mode basis. For the higher one-third octave frequency bands (>315 Hz), where a band-limited power flow approach was featured, reasonable agreement was obtained between measured and predicted noise reduction data. With the interior trim installed the PAIN program seemed to overpredict the noise reduction due to the presence of an airspace between the trim and the interior of the shell surface. SEA predictions agreed well with the measured data (within 3 dB over most of the frequency range of interest) for the simple case of a cylinder bounded by two hard-walled endcaps and an enclosing airspace. SEA predictions were also close to measured data (within 2 dB) for the configuration where the trim was modelled as being directly applied to the interior shell surface.

Introduction

The development and implementation of advanced aircraft designs which use composite materials in their primary structure and incorporate advanced propulsion systems like the advanced turboprop present new challenges for interior noise control in providing an acceptable environment for passengers and crew. Basic experimental acoustic and structural data for such designs is limited.[1-7] This data is needed to gain insight into the phenomena that govern noise transmission and to serve as a data base for validation of interior noise prediction programs. The purpose of the present study is to report on interior noise measurements of a stiffened, floor-equipped, composite cylinder subject to random acoustic excitation. The experimental results are compared with the predictions of two analytical methods. The Propeller Aircraft Interior Noise Program (PAIN)[8-13] predicts a time and space averaged interior sound pressure level in a floor-equipped cylindrical fuselage for a given exterior acoustic excitation. The interior noise levels are determined by the characteristics of the acoustic excitation on the exterior of the fuselage, the coupling of the fuselage structural vibration modes with the interior acoustic modes and by structural and acoustic loss factors. The second prediction method is based on a Statistical Energy Analysis (SEA)[14] which is based on the net power flow of the exterior acoustic energy into the interior acoustic space of the fuselage model. SEA uses modal densities, rather than individual modes, to couple the structural system with the interior acoustic space. To enable comparison between measurements and predictions all data are converted to noise reduction which is defined as the difference between time averaged exterior sound pressure level and space and time averaged interior sound pressure level.

Test Article

The test article used in the current study is a 12 foot filament-wound, stiffened cylinder with a 5.5 foot diameter (figures 1 and 2). The composite material of the cylinder shell consists of graphite fibers embedded in an epoxy resin. The ply sequence was chosen as ±45, ±32, 90, ∓32, ∓45 for a total skin thickness of 0.067 inch. The cylinder is stiffened by 10 J-section ring frames and 22 evenly spaced hat-section longerons. An 0.5 inch thick plywood floor is installed 21.3 inches above the bottom of the cylinder. All elements of the test article are rivet-bonded together. Special endcaps,

* Engineering Specialist, Associate Fellow AIAA

Copyright © American Institute of Aeronautics and Astronautics, Inc., 1989. All rights reserved.

constructed from three layers of 1.25 inch thick particle board with a groove for the cylinder to rest in, provide the boundary conditions at each end. The entire structure is held together by four damped tension rods. An I-beam located along the axis of the cylinder supports a boom on which six microphones are mounted (figure 3). The microphones are located at integral multiples of 5 inches from the centerline. One of the microphones is positioned between the I-beam and the floor. The boom can slide along the center beam which, in turn, can be rotated over 220° to facilitate acoustic measurements at different radial positions in any chosen cross section. As an option, an interior acoustic treatment can be installed (partially shown in figure 2) which consists of a 0.017 inch thick layer of lead sandwiched between two 0.25 inch layers of foam. The treatment is installed on top of the ring frames, leaving a 2 inch airgap between the treatment and the cylinder skin. The total surface weight of the trim is 1.0 lb/ft^2. The foam provides absorption and acts as a decoupler to prevent transmission of structural vibrations from the cylinder shell to the lead layer of the treatment. The treatment is applied to both end-caps without an air gap. The floor is left uncovered.

Experimental Data

Sound Pressure Level Measurements

The composite cylinder and supporting end-caps were placed in the 8000 ft^3 reverberation chamber of the Aircraft Noise Reduction Laboratory at NASA Langley Research Center (figure 1). The cylinder was excited by broadband random noise produced by four loudspeakers, one in each lower corner of the room. The (white) noise signal to the loudspeakers was high-pass filtered at 30 Hz and low-pass filtered at 2000 Hz to encompass the frequency range of interest (100-800 Hz one-third octave bands).

The exterior sound pressure levels were measured using nine microphones mounted on a supporting arc which extended over the upper portion of the cylinder above the location of the floor-shell joints. The microphones were positioned 0.5 inch from the cylinder shell. Nine longitudinal stations were selected to map the exterior sound pressure level distribution. The nine stations were spaced 15 inches apart and were located midway between two ringframes. The first station was located 1 foot from the front end cap. The sound pressure level distribution projected on the unwrapped cylinder shell is shown in figure 4. Only the upper portion of the cylinder, above the floor-shell joints, is unwrapped and interpolation is used on the data leaving the outside borders of the unwrapped portion of the cylinder shell blank. The front end cap is on the left hand side and the bounded horizontal lines are the floor joints. The exterior sound pressure level distribution is shown for two one-third octave bands. They are representative of higher one-third octave bands in that at least 80 percent of the data is within a 3 dB spread of their averaged sound pressure levels.

The interior sound field was measured by the six boom-mounted microphones. The sound pressure level distribution in a crosssection was obtained by measurements with the microphone boom at 15 angular positions, each 15° apart, one of which was in the vertical direction (the 0° position). The cross-section where the measurements were taken was located 36 inches from the front end cap. To map the sound pressure level distributions in the vertical center plane, the boom was positioned at 0° and moved in the longitudinal direction to the 9 stations corresponding to the exterior measurements. The sound pressure level distribution in the horizontal plane was obtained by positioning the microphone boom alternately in the 90° and +90° direction and repeating the sound pressure level measurements for the same nine longitudinal stations as were used to map the vertical plane.

The horizontal, cross-sectional and vertical sound pressure level distributions for the 100 Hz and 125 Hz one-third octave bands are shown in figure 5. The 100 Hz and 125 Hz one-third octave band have a data spread of 15 dB and 14 dB respectively (due to a limited grey scale, areas shown in black or white are not further differentiated). The 100 Hz one-third octave band plot shows the second longitudinal mode which was identified in reference 3 to occur at 94 Hz. The first cross-sectional mode in reference 3 was found at 121 Hz and is shown in the 125 Hz one-third octave band of figure 5. Higher one-third octave bands show similar, but more complex, patterns as the acoustic modal density gets higher.

These interior and exterior sound pressure level measurements were repeated for the case in which the trim was installed inside the cylinder. A space averaging procedure on these sound pressure level measurements was performed to obtain noise reduction values and enable comparison with the prediction methods.

Space Averaged Sound Pressure Levels

The noise reductions predicted by PAIN and the SEA method are based on interior time and space averaged one-third octave band sound pressure levels. Thus, the sound pressure levels inside the cylinder at the measurement locations of the cross-sectional, horizontal and vertical planes have to be reduced to an average interior sound pressure level for each of the one-third octave bands. The average sound pressure level in a reference cross-section, 36 inches from the front endcap, was computed by

$$SPL_{cross} = 10 \log \left[\sum_{m=1}^{M} \sum_{a=1}^{A} \frac{c_m}{M\,A} 10^{SPL_{m,a}/10} \right] \tag{1}$$

where $SPL_{m,a}$ denotes the sound pressure level at the location of microphone m and microphone boom angle a. The index m correspond to the microphone positions depicted in figure 3 with a maximum M=6. The total number of angles, A, equals 15, where a=1 represents -105° from the vertical microphone boom position, a=2 represents -90° and so on in 15° increments. The area correction factor, c_m, corrects for the fact that measurements taken by each of the microphones do not represent equal areas in the cylinder cross section because the microphone spacing on the boom is constant. A reference averaged sound pressure level, SPL_{ref}, was computed from the measurements in the horizontal and vertical directions of the reference crosssection.

$$SPL_{ref} = 10 \log \left[\sum_{m=1}^{M} \sum_{a=1,7,15} \frac{c_m}{M\,R} 10^{SPL_{m,a}/10} \right] \tag{2}$$

where R=3 since the summation is restricted to microphone boom angles of -90, 0, and +90° (a=1, 7, 15).

The average sound pressure level, $(SPL_{long})_n$, of data measured in the horizontal and vertical directions at the other longitudinal stations was calculated. This average sound pressure level is related to the reference averaged sound pressure level by the ratio

$$F_n = \frac{10^{(SPL_{long})_n/10}}{10^{SPL_{ref}/10}} \tag{3}$$

where F_n is the longitudinal sound level factor at station number n. Weighting the averaged sound pressure level of the reference cross-section by F_n results in a representation of the averaged sound pressure level for the entire cross-section at each longitudinal station. Averaging over all nine stations yields the average sound pressure level for the cylinder

$$SPL_{cyl} = \frac{1}{N} 10 \log \left[\sum_{n=1}^{N} F_n 10^{SPL_{cross}/10} \right] \tag{4}$$

The measured exterior (blocked) sound pressure levels were averaged and the noise reduction was computed as the difference between the averaged exterior sound pressure level and the space average interior sound pressure level of the cylinder. The resulting noise reduction is shown in figure 6 as function of the one-third octave band center frequency. The same procedure was repeated for the case where the trim was installed inside the cylinder. The resulting noise reduction for the cylinder with the interior trim is also shown in figure 6.

Loss Factors

Acoustic loss factors were derived from reverberation time measurements at 24 locations inside the cylinder. The reverberation time T is defined as the time for the sound pressure level inside the cylinder to decay through 60 dB after a sound source is abruptly switched off. A loudspeaker was used as the sound source and was placed in one of the corners where the cylinder shell, the floor and the front endcap meet. The acoustic loss factor η was calculated from

$$\eta = \frac{2.2}{f_{1/3} T} \tag{5}$$

where $f_{1/3}$ denotes the one-third octave band center frequency. The structural loss factors were derived in a similar way by measuring the structural reverberation time of the cylinder shell. This reverberation time was obtained from the triggered response of an accelerometer mounted on the cylinder shell after the shell was excited by the impact of a hammer at five different locations. The average structural reverberation time was used to obtain the structural loss factor using equation 5. The structural loss factor is related to the structural damping (for small damping) by

$$\eta = 2 \frac{C}{C_c} \tag{6}$$

where C is the viscous damping coefficient and C_c is the critical damping coefficient. The measured loss factors are tabulated in Table I.

Modal Analysis

An experimental modal analysis was performed to extract resonance frequencies, modal damping and mode shape coefficients of the composite cylinder. Frequency response functions were obtained from accelerometer measurements that were normalized to the impulse excitation from a modal hammer. Acceleration response locations included 22 evenly spaced shell locations in cross sections at one-half and one-third the cylinder length. In the longitudinal direction acceleration response was measured at 19 evenly spaced shell locations 90 degrees and 155 degrees from the bottom of the cylinder. Impulse excitation was applied at two reference locations where the 155 degrees longitudinal intersects with the two response cross sections. A poly reference complex exponential technique was used to simultaneously manipulate response functions for both reference locations to yield the desired modal parameters.

Several structural modes were identified in the frequency region below 250 Hz and are tabulated in Table 2 along with their modal damping. The mode number identifies the mode by the number of half-waves in the longitudinal direction (l) and the number of waves in the circumferential direction (c). The type of mode is either symmetric (S) or antisymmetric (A) depending on its mode shape in relation to the vertical through the center of a cylinder cross section. Note that the modal damping in Table 2 is for individual modes while the loss factors in Table 1 are for the one-third octave bands which comprise the contribution of multiple resonant and non-resonant responses. Above 250 Hz it becomes increasingly more difficult to separate the response of the individual modes as the modal density gets higher. Acoustic modal frequencies were identified previously and are tabulated in Table 2 of reference 3.

Interior Noise Predictions

PAIN

The Propeller Aircraft Interior Noise computer program was developed to predict the time and space averaged sound pressure level inside propeller driven aircraft due to exterior acoustic excitation.[8-13] The model is based on the principle of power flow balance, which equates the band-limited net time-averaged power flowing into the cylinder's interior to the band-limited net time-averaged power dissipated on the cylinder walls. At low frequencies, where the acoustic modal density is low, the power flow from each structural mode of the cylinder into each acoustic mode of the interior, resonant as well as non-resonant, is computed. Similarly, the power flow from the interior acoustic field into the cylinder wall is computed on a mode per mode basis. At frequencies where the acoustic modal density is high the transmission is expected to be dominated by modal resonance response and, therefore, only band-limited structural modes close to the excitation frequency are considered. The frequency at which to change from the low modal density formulation to the high modal density formulation can be set in the computer program. The PAIN program was originally designed to accept the magnitude and phase of tonal excitation caused by the rotation of a propeller. However, modification to the program allows noise reduction calculations for the condition where the test article is excited by a reverberant (diffuse) acoustic field. The noise reduction is defined as the difference between the exterior blocked sound pressure level (which is assumed to be constant for all locations on the cylinder surface) and the time and space averaged interior sound pressure level. The modal damping of the cylinder, without the trim, and its interior acoustic space is not calculated by the PAIN program and must be input as acoustic and structural loss factors. When an interior trim is installed, the acoustic loss factor for the interior is, at low frequencies, calculated for each individual acoustic mode. At high frequencies an average loss factor is analytically derived for specified one-third octave bands. A trim loss factor, which arises because of flexure of the trim lining, has to be estimated and is an input into the PAIN program. The trim loss factor is needed to calculated the trim transmission coefficient. Contributions to the interior noise due to mechanical vibration transmission from cylinder skin to trim panel is included by a mechanical transmission coefficient. This mechanical transmission coefficient is derived using statistical energy analysis procedures and includes, among other parameters, the trim loss factor and a coupling loss factor describing the transmission loss from the skin to the trim. The coupling loss factor, which depends on how the skin and trim are connected, is calculated. The current version of the PAIN program is capable of handling a floor inside the cylinder and analyzing composite material properties. The boundary conditions of the floor-shell joints are considered to be simply supported.

SEA

In Statistical Energy Analysis[14] the structure under consideration is composed of subsystems, each containing vibratory or acoustic energy and each interacting and exchanging energy with neighboring subsystems. Power balance equations can be set up to describe the power flow from one subsystem to all connected subsystems the sum of which equals the power injected into that subsystem minus any dissipated power. The principle of the SEA method is that the net power flow between two coupled (sub)systems in a narrow frequency band centered at frequency f is proportional to the difference in the modal energies of the two subsystems at the same frequency. The power flow is from the (sub)system with the higher modal energy to that with the lower modal energy. For the present study the composite cylinder is modelled as a composite of four subsystems, a composite cylindrical shell, two hard-walled end caps and an interior acoustic space. The blocked sound pressure level measured on the exterior of the cylinder has been converted to acoustic power for input into the shell subsystem. Both the cylinder geometry and the material properties of the composite skin are input in the analysis. The longitudinal wave speed in the shell is calculated from the material properties and used to compute the critical frequency and ring frequency of the cylinder model. Also included in the input are the properties of the acoustic medium and the measured structural and acoustic loss factors. To model the cylinder with the interior trim installed, the mass of the trim is added to the shell subsystem and the acoustic loss factors are calculated from the absorption coefficients as given by the manufacturers product data sheet.

Comparison of Measurements and Predictions

Noise Reduction of the Bare Cylinder

PAIN Predictions.- The PAIN program calculates first the structural and acoustic modes in separate subprograms. For the computation of the structural modes the geometry and material properties of the cylinder, the ring frames, longerons, floor and floor supports were input into the subprogram. A surface weight of 0.55 lb/ft^2 was used for the composite shell and 1.84 lb/ft^2 for the plywood floor. The material properties of the graphite fibers and epoxy of the composite shell were estimated from similar materials used in another study.[15] The program was set to calculate cylinder modes to a maximum mode number of 15 in the longitudinal direction and 14 along its circumference. Floor modes were calculated up to a maximum mode number of 15 in the longitudinal direction and a maximum mode number of 14 along its width. This resulted in the calculation of a total of 432 structural modes up to and including the 800 Hz one-third octave band. The one-third octave band distribution of the number of modes over the frequency range of interest (100 Hz - 800 Hz) is given in Table 3. Below the 100 Hz one-third octave band 32 modes were calculated. A total of 352 acoustic modes were computed from cylinder geometry input data and the location of the floor in the cylinder. The number of acoustic modes in each one-third octave band is also tabulated in Table 3. The PAIN program then combines the structural and acoustic modal information with the input of the experimental loss factors (Table 1) to compute the structural-acoustic coupling factors, the net power flow into the interior and finally the noise reduction of the bare cylinder. The frequency at which to change from the low modal density to the high modal density formulation was set at 400 Hz in the computer program. This frequency was chosen as 41 acoustic modes were calculated to be resonant in the 400 Hz one-third octave band which is high enough to assume that noise transmission is dominated by band-limited modal response. The PAIN predicted noise reduction is compared with the measured noise reduction in figure 7. Reasonable agreement is obtained for the 315 Hz and higher one-third octave bands. For the lower frequency bands, however, the PAIN predicted noise reduction differs considerably from the experimentally obtained values. In these bands the power flow from each structural mode into each acoustic mode, resonant as well as non-resonant, is calculated. The predicted noise reduction is thus dependent on how well these structural and acoustic modes are predicted. Although many coupled acoustic and structural modes are included in the calculation of the interior noise in each frequency band, the output of the PAIN program shows five coupled acoustic and structural modes that contribute the most to the interior sound field.

For the discussion here the most dominant coupled modes in each of the five lowest one-third octave are tabulated in Table 4. In the 100 Hz one-third octave band the (2,0,0) acoustic mode (number of half-waves in longitudinal, horizontal, and vertical directions, respectively) is coupled to the (1,2) symmetrical structural shell mode (number of half-waves longitudinally and number of waves along the circumference). The PAIN predicted acoustic mode shows good agreement with the measured acoustic mode (from reference 3). However, the (1,2) shell mode was predicted at 108.9 Hz and measured at 62 Hz. In the 125 Hz one-third octave band reasonable agreement was obtained for the predicted and measured (1,1,0) acoustic modes. This acoustic mode couples with a (1,2) floor mode at 93.7 Hz. This mode was not identified by the experimental modal analysis. From Table 4 it can be seen that for the other three one-third octave bands the acoustic modes are predicted fairly accurately while the structural modes to which they are coupled are wrongly predicted. The inability of the PAIN program to accurately predict these structural modes is not necessarily due to incorrect analytical assumptions. For a complex structure as the current test article with a composite skin, discrete composite stiffeners and longerons, and a supported plywood floor several input parameters had to be estimated including composite and plywood material properties, and the boundary conditions at the shell-floor joint. Also, different ways in modelling the discrete stiffeners and longerons, which are rivet-bonded onto the cylinder shell, and the floor supports cause variations in the parameters that the PAIN program uses to predict the structural modes. Since these parameters all interact there is no simple relationship between them and the resulting structural modal parameters which makes it impossible to explain the disagreement with experimental data without an extensive sensitivity study. A Statistical Energy Analysis has been performed to predict the noise reduction of the composite cylinder without the use of individual structural (and acoustic) modes.

SEA Predictions.- For the SEA predictions the test article was modelled as a cylinder with a composite shell with a surface mass of 0.55 lb/ft^2, bounded by two hardwalled endcaps and an interior acoustic space. The same experimental acoustic and structural loss factors (Table 1) were used as were input for the PAIN predictions. The resulting noise reduction is depicted in figure 7. Except for the 125 Hz one-third octave band the data spread is within 3 dB of the measured noise reduction for the bare cylinder. Even at the lower acoustic modal densities in the 100 Hz - 250 Hz one-third octave bands (Table 3) the SAE predictions are reasonably close to the measured data. This may in part be due to the large number of structural modes that participate in the sound transmission in these frequency bands (Table 3). The data in figure 7 suggest that the advantage of PAIN to predict noise reduction at frequencies where the modal density is low is lost when the modes participating in the sound transmission are not predicted correctly.

Noise Reduction of the Cylinder with the Trim Installed

PAIN Predictions.- For input into the PAIN program the interior treatment was modelled as a 0.017 inch thick layer of lead on top of a 0.5 inch thick layer of foam with a 2 inch airgap between the foam and the interior shell surface. The total surface weight of the trim was 1.0 lb/ft^2. As for the bare cylinder, noise reduction predictions were chosen to change from the low modal density to the high modal density formulation in the 400 Hz one-third octave band. A trim loss factor, which arises because of flexure of the lining, was arbitrarily chosen to have a value of 0.4 (the trim loss factor equals 2.0 for the case of critical damping). The PAIN noise reduction predictions for the composite cylinder with the trim installed are compared with the measured data in figure 8. The PAIN results overpredict the measured noise reduction in the 100 Hz - 500 Hz one-third octave bands. Part of this, of course, is due to disagreement in the predictions for the bare cylinder. To investigate the effect of trim by itself, the increase in noise reduction due to the installation of the trim is plotted in figure 9 for both the predicted and measured results. Although much better agreement is obtained in the 100 Hz, 125 Hz, and 160 Hz one-third octave bands, PAIN still overpredicts in the higher one-third octave bands up to and including the 500 Hz band. To investigate which part of the trim treatment caused this overprediction the PAIN program was run without the 0.5 inch thick foam layer. The effect of the foam was negligible in the frequency range of interest as noise reduction predictions did not change by more than 1 dB for this configuration. PAIN predictions were then obtained for the configuration in which the trim septum of lead was directly applied to the shell. As shown in figure 9, the predicted increase in noise reduction is now within 4 dB of the measured increase in noise reduction except for the 315 Hz one-third octave band where PAIN underpredicts by about 7 dB. As the trim loss factor (TLF) was arbitrarily chosen to have a value of 0.4, the effect of this input parameter has been investigated by changing its value to 1.0 and 0.2, respectively, for the case of the lead trim septum being directly applied to the shell. The predicted increase in noise reduction due to these different values of the trim loss factor is depicted in figure 10. Its behavior can be roughly defined to be 10 log (TLF) for the entire frequency range of interest except for the 100 Hz one-third octave band. As the effect of the trim loss factor on the increase of noise reduction due to the trim is deterministic and constant over most of the frequency range of interest, it can be concluded from the data presented in figures 8-10 that the PAIN program overpredicts the effect of the airspace that separates the septum from the skin. To verify this conclusion a Statistical Energy Analysis was performed for the case of the trim septum directly applied to the skin.

SEA Predictions.- A Statistical Energy Analysis was performed for the composite cylinder with the trim, which has a surface mass of 1.0 lb/ft^2, directly applied to the skin of the shell. Absorption coefficients, as supplied by the manufacturer, were input in the analysis. The predicted noise reduction is plotted in figure 8 and is within 2 dB of the measured noise reduction data over the entire frequency of interest. Combined with the analysis of the PAIN predictions this suggests that the 2 inch airgap between the trim and the cylinder shell provides little or no noise reduction for the frequency bands considered.

Concluding Remarks

Interior and exterior measurements were conducted for a composite, floor-equipped, cylinder subjected to random acoustic excitation, with and without an interior trim installed. The noise reduction derived from these measured data was compared with the noise reduction predicted by the Propeller Aircraft Interior Noise (PAIN) program and by a Statistical Energy Analysis (SEA). With the input data provided the PAIN program did not compute the structural modal response correctly which resulted in incorrect noise reduction values for frequencies where the power flow into the cylinder was computed on a mode per mode basis. Reasonable agreement in noise reduction values was obtained for the higher one-third octave bands (>315 Hz) where the modal density was high and the power flow was computed on a one-third octave band limited basis. The inability to predict the structural modal response was not necessarily attributed to inaccuracies in the analytical formulation, but was also attributed to incorrect estimation of the input parameters like material properties and boundary conditions. For the configuration where the trim was installed in the interior of the cylinder, the PAIN program overpredicted the effect of a 2 inch spacing between the trim and the interior shell surface for the frequency region of interest (100 Hz - 800 Hz). The predictions of the Statistical Energy Analysis were generally within 3 dB of the measured data for the bare cylinder and within 2 dB for the configuration with the trim installed directly to the interior of the cylinder shell. A sensitivity study is recommended to investigate the discrepancies of the PAIN predictions with the measured structural modal parameters and to investigate the effect of the 2 inch air space between the trim and the interior shell surface.

Acknowledgements

This research was supported by NASA Langley Research Center, Contract NAS1-18000, Dr. C. A. Powell, Technical Monitor.

References

[1] Bray, F. M.; and Egle, D. M.: An Experimental Investigation of the Free Vibration of Thin Cylindrical Shells with Discrete Longitudinal Stiffening. Journal of Sound and Vibration, vol. 12, 1970, pp. 153-164.

[2] Koval, L. R.: Sound Transmission into a Laminated Composite Cylindrical Shell. Journal of Sound and Vibration, vol. 71, no. 4, 1980, pp. 523-530.

[3] Grosveld, F. W.; and Beyer, T. B.: Modal Characteristics of a Stiffened Cylinder with Open and Closed End Conditions. AIAA Paper No. 86-1908, 10th Aeroacoustics Conference, Seattle, Washington, July 9-11, 1986.

[4] Beyer, T. B.; and Grosveld, F. W.: Validation of an Interior Noise Prediction Model for a Composite Cylinder. AIAA Paper No. 87-0529, 25th Aerospace Sciences Meeting, Reno, NV, January 12-15, 1987.

[5] Grosveld, F. W.; and Beyer, T. B.: Vibratory Response of a Stiffened Floor-Equipped, Composite Cylinder. Conference Proceedings of the 5th International Modal Analysis Conference, London, England, April 6-9, 1987, pp. 812-820.

[6] Marulo, F.; and Beyer, T. B.: NASTRAN Application for the Prediction of Aircraft Interior Noise. 1987 NASTRAN Users Colloquium, Kansas City, Missouri, May 4-8, 1987.

[7] Grosveld, F. W.; Sullivan, B. M.; and Marulo, F.: Aircraft Interior Noise Prediction Using a Structural-Acoustic Analogy in NASTRAN Modal Synthesis. Conference Proceedings of the 6th International Modal Analysis Conference, Orlando, Florida, February 1-4, 1988, pp. 1191-1198.

[8] Pope, L. D.; Wilby, E. G.; and Wilby, J. F.: Propeller Aircraft Interior Noise Model. NASA CR 3813, July 1984.

[9] Pope, L. D.; Rennison, D. C.; Willis, C. M.; and Mayes, W. H.: Development and Validation of Preliminary Analytical Models for Aircraft Interior Noise Prediction. Journal of Sound and Vibration, vol. 82, no. 4, 1982, pp. 541-575.

[10] Pope, L. D.; Wilby, E. G.; and Wilby, J. F.: Propeller Aircraft Interior Noise Model, Part I: Analytical Model. Journal of Sound and Vibration, vol. 118, no. 3, 1987, pp.449-467.

[11]Pope, L. D.; Willis, C. M.; and Mayes, W. H.: Propeller Aircraft Interior Noise Model, Part II: Scale-Model and Flight-Test Comparisons. Journal of Sound and Vibration, vol. 118, no. 3, 1987, pp. 469-493.

[12]Pope, L. D.: Propeller Aircraft Interior Noise Model - Utilization Study and Validation. NASA CR 172428, September 1984.

[13]Wilby, E. G.; and Pope, L. D.: Propeller Aircraft Interior Noise Model - User's Manual for Computer Program. NASA CR 172425, January 1985.

[14]Ver, I. L.; and Holmer, C. I.: Interaction of Sound Waves with Solid Structures. Noise and Vibration Control, Beranek, L. L. (Ed.), McGraw-Hill Book Company, 1971.

[15]Roussos, L. A.; Powell, C. A.; Grosveld, F. W.; and Koval, L. R.: Noise Transmission Characteristics of Advanced Composite Structural Materials. Journal of Aircraft, vol. 21, no. 7, 1984, pp. 528-536.

TABLE 2. EXPERIMENTAL STRUCTURAL MODAL PARAMETERS

Modal Frequency [Hz]	Mode Shape	Type l,c	Modal Damping C/C_c
52	1,2	A	0.0684
62	1,2	S	0.0391
89	1,3	A	0.0128
96	2,2	S	0.0258
106	2,3	A	0.0169
137	1,4	A	0.0147
151	2,4	A	0.0179
159	3,3	A	0.0176
197	3,5	A	0.0105
206	2,5	A	0.0188
219	3,4	S	0.0082
228	2,6	A	0.0172
249	1,6	S	0.0065
252	2,6	S	0.0168

l = longitudinal
c = circumferential
A = antisymmetric
S = symmetric

TABLE I. MEASURED ACOUSTIC AND STRUCTURAL LOSS FACTORS

1/3 Octave Band Center Frequency [Hz]	Acoustic Loss Factors	Structural Loss Factors
100	0.013	0.0590
125	0.023	0.0352
160	0.049	0.0293
200	0.019	0.0271
250	0.012	0.0236
315	0.010	0.0248
400	0.006	0.0110
500	0.006	0.0094
630	0.006	0.0112
800	0.005	0.0098

TABLE 3.- PAIN PREDICTED NUMBER OF STRUCTURAL AND ACOUSTIC MODES

One-Third Octave Band [Hz]	Number of Modes: Structural	Number of Modes: Acoustic
<100	32	2
100	23	1
125	21	3
160	23	3
200	22	7
250	28	10
315	32	23
400	43	41
500	56	77
630	63	93
800	89	92

TABLE 4.- PAIN PREDICTED COUPLING OF ACOUSTIC AND STRUCTURAL MODES

One-Third Octave Band [Hz]	Acoustic Modes Number l, h, v	Acoustic Modes Frequency [Hz] PAIN	Acoustic Modes Frequency [Hz] Measured*	Structural Modes Number l,c	Structural Modes Type	Structural Modes Frequency [Hz] PAIN	Structural Modes Frequency [Hz] Measured
100	2,0,0	93.8	94	1,2	S	108.9	62
125	1,1,0	124.6	121	(Floor Mode)		93.7	---
160	2,1,0	148.7	150	3,5	A	164.9	197
200	3,1,0	182.0	183	2,3	A	189.2	106
250	1,2,0	222.7	230	2,3	A	189.2	106

l = longitudinal
h = horizontal
v = vertical
c = circumferential
A = antisymmetric
S = symmetric

* reference 3

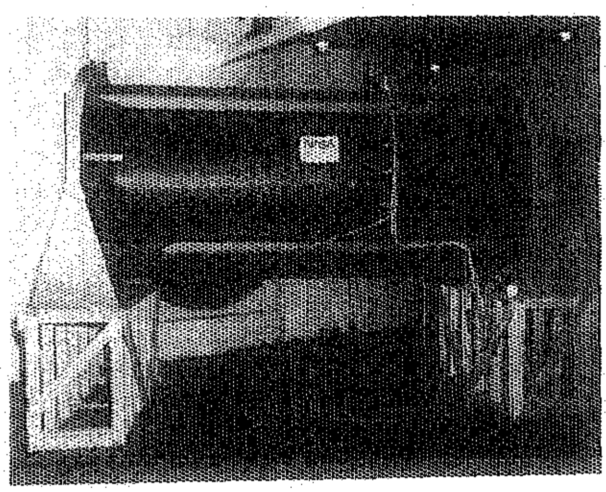

Figure 1. Composite cylinder in the reverberation chamber.

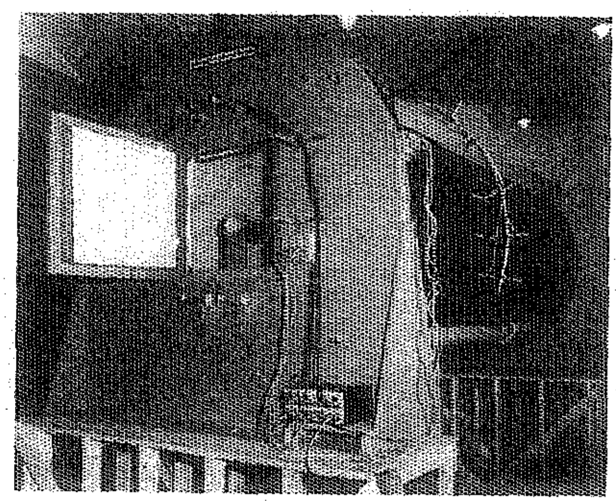

Figure 2. Front end cap of the composite cylinder with open access door partially showing the optional interior trim.

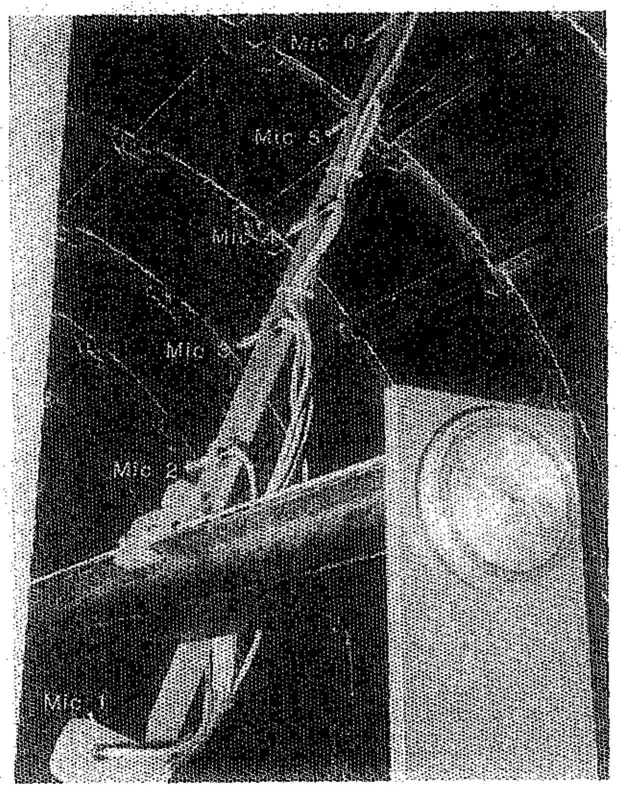

Figure 3. Microphone boom used for acoustic data acquisition.

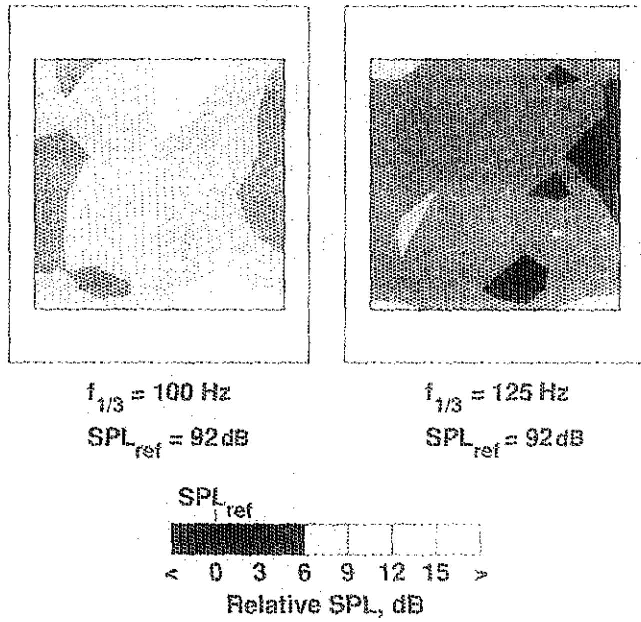

Figure 4. Exterior sound pressure level distribution projected on the upper unwrapped portion of the cylinder shell between the two floor joints. Front end cap is on the left.

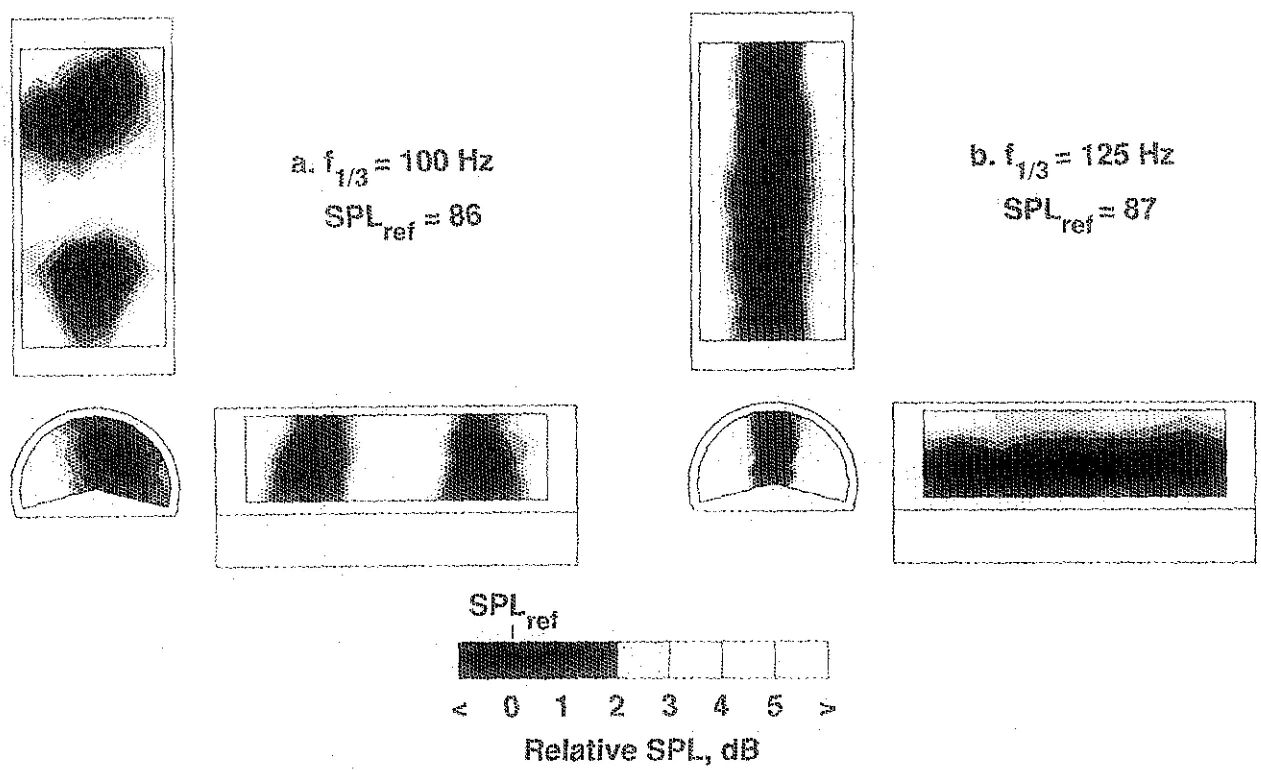

Figure 5. Horizontal, vertical, and cross-sectional interior sound pressure level distributions for the bare composite cylinder.

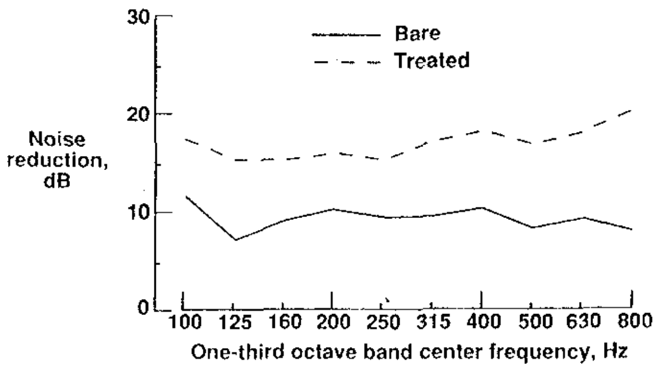

Figure 6. Measured noise reduction for the bare composite cylinder and with interior trim installed.

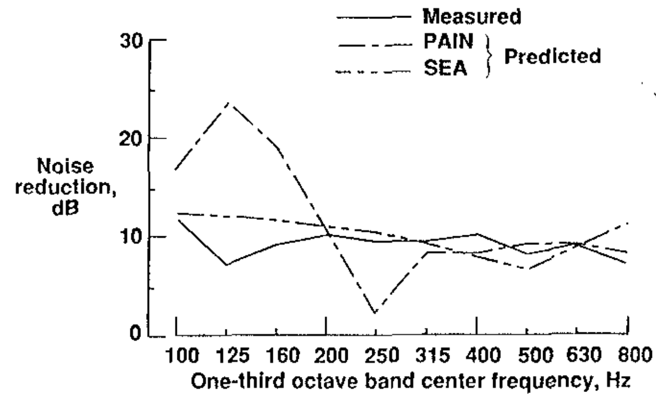

Figure 7. Measured and predicted noise reduction for the bare composite cylinder.

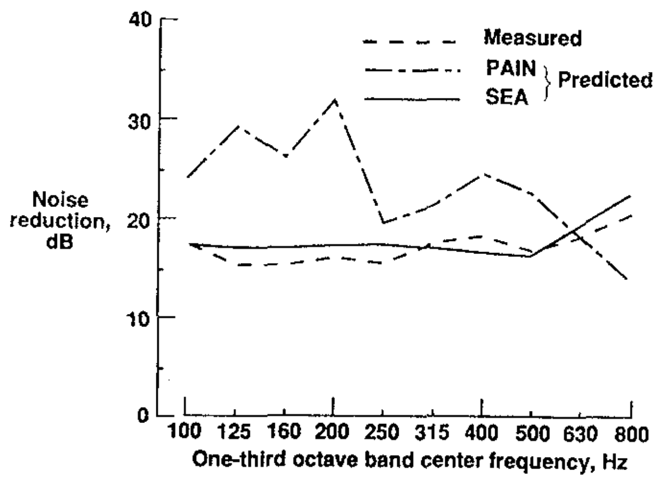

Figure 8. Measured and predicted noise reduction for the composite cylinder with the trim installed.

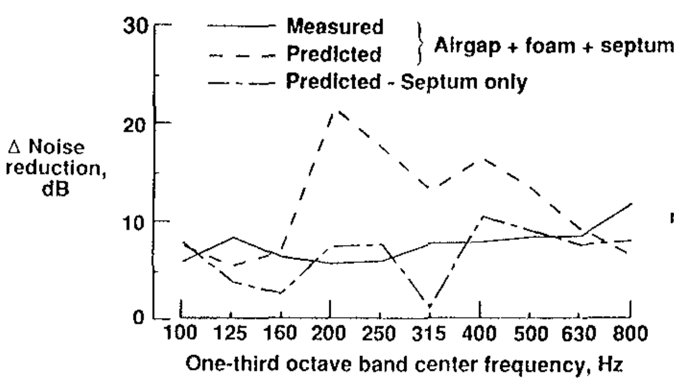

Figure 9. Measured and PAIN predicted increase in noise reduction due to the installation of an interior trim.

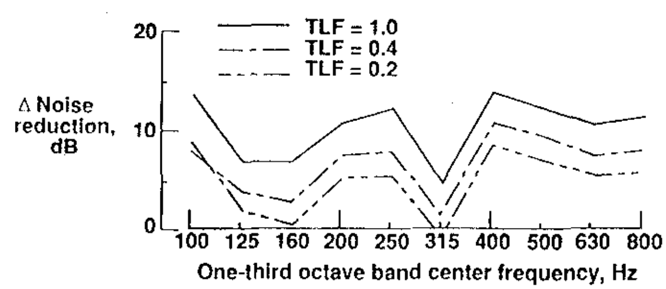

Figure 10. Effect of the trim loss factor (TLF) on the predicted increase in noise reduction due to the installation of a trim septum.